

OPTICAL PROPERTIES OF FIBROUS BRUCITE FROM ASBESTOS, QUEBEC

RICHARD S. LIEBLING, *Department of Geology and Geography,
Hunter College of the City University of New York, New York 10021*

AND

ARTHUR M. LANGER, *Environmental Sciences Laboratory,
Mount Sinai School of Medicine of the City University
of New York, New York 10029*

ABSTRACT

Fibrous brucite, commonly referred to in the literature as nemalite, from Asbestos, Quebec, is indistinguishable from platy brucite when compared by powder X-ray techniques. Chemical analyses of the lath-like fibers show them to be significantly higher in iron, manganese, and silicon as compared to the platy brucites. Iron and manganese substitution for magnesium readily explains high refractive indices. Brucite laths possess a biaxial interference figure in contrast to the uniaxial figure observed on plates. Electron microscopy and selected area diffraction on small laths suggest that the optical biaxial figure may have formed as the result of a co-axial growth of chrysotile fibrils (which accounts for the silicon) and laths of brucite. This intergrowth could explain the formation of lath aggregates disoriented with respect to the fiber axis. Prismatic cleavage is markedly visible under the electron microscope.

INTRODUCTION

Fibrous brucite (frequently referred to in the literature as nemalite) was collected at Asbestos, Quebec, where it occurs in shear zones as thick masses of long aggregate fibers associated with chrysotile. The strong association of chrysotile and brucite, their co-axial growth and the intermixed nature of the fibers, has suggested that brucite formed as a result of replacement of chrysotile (Berman, 1932). Brucite fibers in this area are uncommonly high in iron and such species have been referred to as ferrobrucite (Ford, 1932, p. 508). Platy and fibrous brucites from this locality were compared and a biaxial optical figure and higher refractive indices were observed in the nemalite variety. The nature of the characteristics is discussed.

X-RAY DIFFRACTION

Specimens of fibrous brucite were examined with both the X-ray diffractometer and the Debye-Scherrer powder camera. X-ray patterns obtained with the diffractometer were too highly oriented with respect to the fiber (a_1) axis to obtain a set of reflections for comparison with standards. The powder camera pattern obtained was es-

sentially the same as that reported in the XPDF for platy brucite: no magnetite, limonite, or other iron-bearing substances were detected, even though fluorescence had darkened the film considerably. No other contaminants were observed by X-ray examination.

CHEMICAL COMPOSITION

Berman (1932) reported that fibrous brucite contains substantial amounts of iron. Our preliminary emission spectrography showed that the fibrous brucite contained, in order of abundance, magnesium, iron, manganese, and silicon. Standard wet chemical analysis followed (Table 1). The silica content was recalculated with appropriate amounts of water and magnesia to form chrysotile (Table 1, Column 4). The chrysotile contamination, clearly visible by electron microscopy, was not detectable by light microscopic examination.

The corrected chemical analysis shows a 7 percent "excess" of divalent cations (Table 1, Column 7). Although this "excess" was previously explained by impurities, a preliminary electron microprobe study of the fibers showed a homogeneous Fe distribution in the brucite laths. Five to eight percent iron was calculated as being present structurally. Transmission electron microscopy also contraindicated iron mineral contaminants, as did the X-ray examination. It may be that some of the hydroxyl groups have been replaced by oxygens, as is common in hydrated minerals.

Table 1: CHEMICAL ANALYSES OF BRUCITE

Oxide	(1)	(2)	(3)	(4)	(5)	(6)	(7)
SiO ₂	1.13	1.13
MgO	69.11	60.33	61.72	1.14	60.58	60.58
FeO	11.52	8.70	8.70	1.91	7.03
MnO	0.24	0.24		
H ₂ O	30.89	28.60	28.27	0.34	27.93	27.93
Total	100.00	100.45	100.06	2.61	97.45	90.42	7.03

(1) Mg(OH)₂.

(2) Analysis of fibrous brucite from Berman (1932). Total iron given here as Fe²⁺, original analysis cites both ferrous and ferric content.

(3) Analysis of fibrous brucite, this study. Fe and Mn determined by AAS, errors of 0.15 and 0.03 percent respectively; Mg determined by the ammonium phosphate method with an error of 0.20 percent; Si and H₂O determined gravimetrically, errors of 0.05 and 0.20 percent respectively.

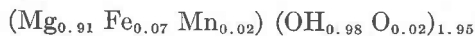
(4) Silica content recalculated into chrysotile with appropriate amounts of magnesia and water.

(5) Brucite analysis without chrysotile components.

(6) Brucite calculated on the basis of water content as completed anion structure. All the magnesia "fits" into the structure but only 1.9 percent of the other divalent cations can be used to satisfy charge requirements.

(7) Divalent cation "excess".

Recalculating mole percents for a complete structural accommodation of cations, the representative formula would be as follows:



OPTICAL CHARACTER OF FIBROUS BRUCITE

On the light microscope level, the fibrous brucite appears to consist of aggregates of laths which may readily subdivide on manipulation (Fig. 1). Between crossed nicols, apparently single laths are almost isotropic and rarely show interference color above first order white. The elongation is negative and as brucite is uniaxial positive, the lath axis cannot be *c*. This feature was noted by Berman (1932).

On selected single laths, those with no refringence or relief change on rotation, the index of refraction, ω , was determined parallel and perpendicular to the lath length. Values of 1.577 (3) and 1.575 (5) were obtained respectively. These are identical. These values compare to the literature as follows:

	(1)	(2)	(3)	(4)	(5)
ω	1.562	1.566	1.559	1.585*	1.576*
ϵ	1.582	1.585	1.580		
$\omega - \epsilon$	0.020	0.019	0.021		

- (1) Ford (1957, p. 508)
- (2) Rogers and Kerr (1942, p. 205)
- (3) Larsen and Berman (1934, p. 70)
- (4) Berman (1932, p. 70)
- (5) This study (average)

The mean refractive index is representative of ω . Although a small component of ϵ may have been measured, it is considered negligible on the basis of lath selection. The high value obtained for ω is attributed to the moderate iron and manganese in the structure.

The interference figure, as determined in the plane of the lath, is not uniaxial, but appears to be *biaxial* and diffuse. No $2V$ value was obtained. Berman (1932) did obtain $2V = +70^\circ$, and attributed it to a precession of *c*-axes produced as crystals are stacked in the laths. Lath axes (fiber axes) appear to be, at least, subparallel on the basis of extinction properties.

ELECTRON MICROSCOPY AND SELECTED AREA DIFFRACTION

Specimens were prepared for electron microscopy by "teasing" the

* Index measured on component vibrating in plane of lath.

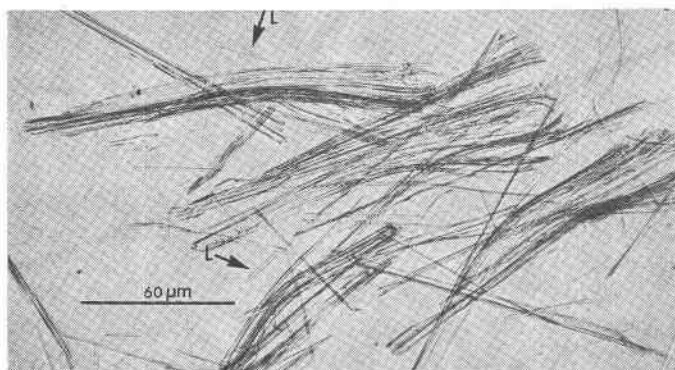


FIG. 1. Fibrous brucite as seen in plane polarized light. Clearly defined laths are marked (L) by arrows. Note lower lath is terminated by a prism.

fibers onto Formvar-coated 200-mesh copper grids. They were examined with an RCA EMU-3G electron microscope at 100 kV. At high magnification, the aggregate fibers are composed of elongated lath-like crystals with perfect to imperfect prism cleavage terminations. These are morphologically identical to the brucite laths visible by light microscopy. Many of the brucite laths have first- and second-order prisms and some have irregular right-angle terminations (Figs. 2, 3, 5). Interspersed among the laths are sub-light microscopic chrysotile fibrils (fibers are rare) which range in length and width (Fig. 3). The chrysotile fibril is some 300–450 Å in width and represents the limit of individual unit growth. The fiber is made up of many unit

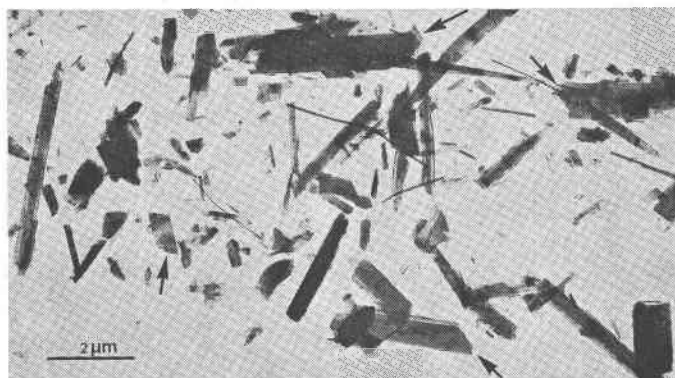


FIG. 2. Transmission electron micrograph of fibrous brucite. Many of the brucite laths show prism cleavage terminations (arrows). Small fibers in background, with widths less than 0.05 μm , are chrysotile.

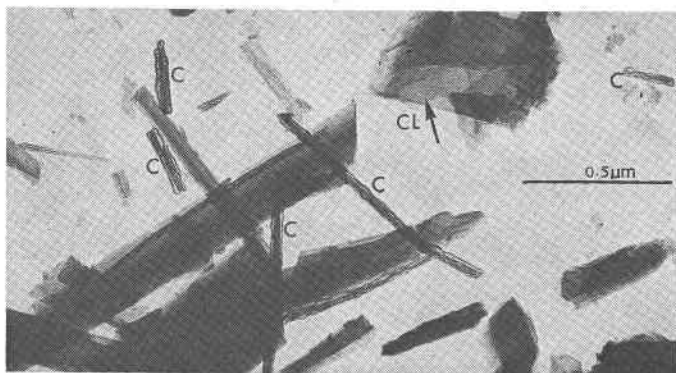


FIG. 3. Transmission electron micrograph of brucite laths and associated chrysotile. Prismatic cleavage of brucite is marked (CL); beam-damaged chrysotile fibrils (C).

fibrils which grow into contact. In many instances, the chrysotile fibrils may be observed directly on the brucite laths, with parallel axial growth (Fig. 4). Chrysotile intergrowths are almost restricted to fibril-sized units.

SELECTED AREA DIFFRACTION

With electron diffraction it is possible to obtain a direct section of the reciprocal lattice on a flat plate normal to the electron beam. With a Laue geometry (fixed film and crystal), both dimension and angle characteristics may be directly measured (McConnell, 1967). Grids prepared for transmission electron microscopy were used for diffraction on single laths (Fig. 5).

Values of 3.07 (4) Å and 5.32 (7) Å were measured for a and $a\sqrt{3}$ respectively. These correlate well with 3.12 Å and 5.38 Å given by Bragg and Claringbull (1965, p. 116). Reflections of the (000 l) plane are sharp and regular. On the basis of comparative electron densities the laths which yielded these patterns were up to 400 Å in thickness and were obtained on at least 80 unit cells. Berman (1932, p. 314-315) obtained single crystal photographs (both by rotation and Laue methods) of a brucite fiber and observed the "aggregate is not in parallel orientation across the elongation of the fibers". The biaxial figure he observed was attributed to the "deviation of the c -axes of the individual laths making up the aggregate".

DISCUSSION

Brucite normally occurs as foliated, platy masses or as tabular crystals. The fibrous form (nemalite) is much less common and, from

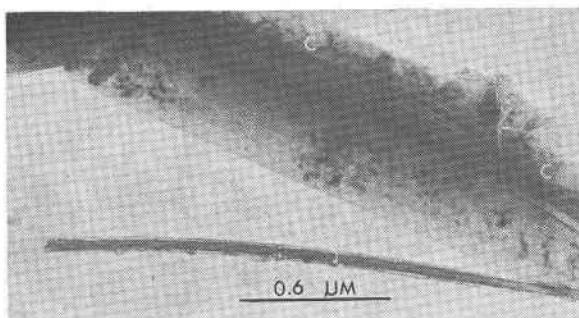


FIG. 4. High magnification view of chrysotile fibrils (C) on the surface of a brucite lath. Parallel axial growth of the minerals is common.

the data available, high in iron. Examination of fibrous brucite by X-ray powder diffraction shows it to be indistinguishable from normal platy brucite. The index of refraction is higher than values reported for platy brucite, a function of the high iron and manganese substitution.

Laths separated from aggregate fibers show a diffuse biaxial figure. Berman (1932) was able to measure this and explained the figure on the basis of an "aggregate fanning" of *c* axes of crystals in a plane perpendicular to the fiber (and lath) axis. This was supported by his X-ray data. Data obtained in this study, by light microscopy and electron diffraction, show the presence of the biaxial figure, but show no such disorientation effect by diffraction examination.

The optical data cited by Berman, and in the present study, were obtained on laths which appeared to be single crystals. These may in truth have been "aggregates". The single crystal X-ray data cited by Berman was obtained on an aggregate fiber, as indicated by his own terminology (p. 315). However, no specific mention is made of fiber dimension in that paper. The single crystal data cited in the present study were obtained on laths just at the lower limits of resolution by light microscopy. These are smaller in size than comparable crystals examined by Berman, and are true single crystals.

The sub-light microscopic intergrowths of chrysotile parallel to the lath fiber axis can account for the observed disorder in the relatively large laths which, although they appear to be single crystals, are in truth aggregates of crystals. However, another explanation is also possible. Brucite's changed morphology may reflect a more fundamental structural modification. The accuracy of the electron diffraction method is such that small lattice distortions may go unresolved. If this is the case, the biaxial figure may reflect the existence of a

lower symmetry structural polymorph of brucite. The undistorted figures obtained by this method on the laths, would be pseudo-hexagonal, as is commonly observed on clays and micas by the same method. Although microscopic intergrowths of chrysotile between brucite laths is at present the most reasonable explanation for the apparent stacking disorder of crystals in aggregate laths, further investigation is required for a unique solution.

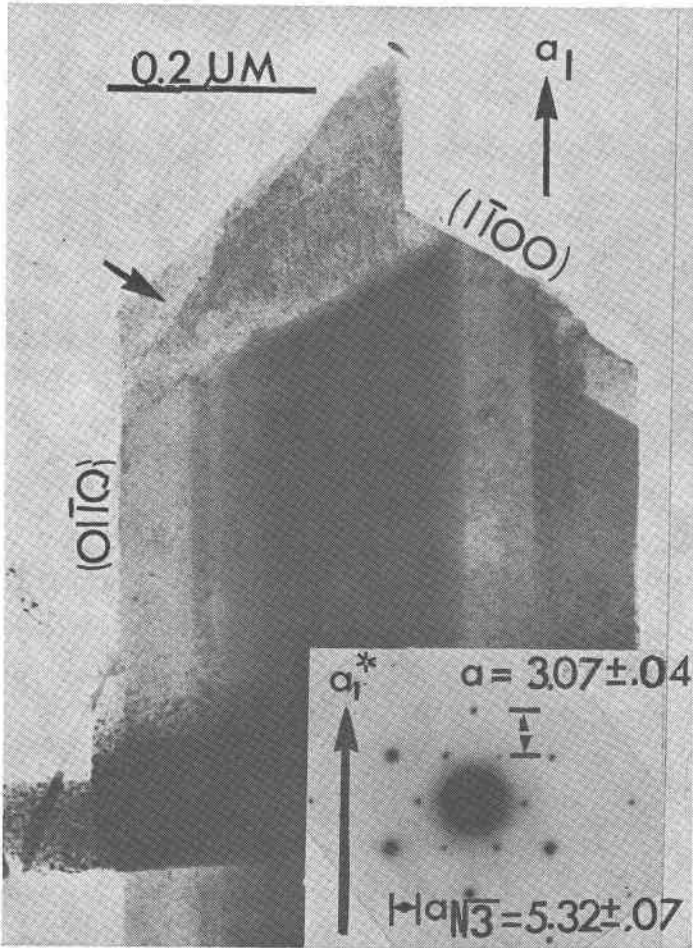


FIG. 5. Brucite lath and its accompanying electron diffraction pattern. Micrograph and pattern are shown with a and a^* parallel. Camera constant at 100 kV is about 35.54 ($L\lambda$). Cleavages are marked. Arrow indicates a possible imperfect second-order prismatic cleavage (1120).

ACKNOWLEDGMENTS

One of us (AML) wishes to acknowledge support under Career Award NIEHS ES 44812.

REFERENCES

- BERMAN, H. (1932) Fibrous brucite from Quebec. *Amer. Mineral.* 17, 313-316.
- BRAGG, W. L., G. F. CLARINGBULL, AND W. H. TAYLOR (1965) *Crystal Structures of Minerals*. G. Bell and Sons, Ltd., London, 409 p.
- FORD, W. E. (1932) *Textbook of Mineralogy of E. S. Dana, 4 ed.* John Wiley and Sons, N. Y., 851 p.
- LARSEN, E. S., AND H. BERMAN (1934) The microscopic determination of non-opaque minerals. *U. S. Geol. Surv. Bull.* 848, 266 p.
- MCCONNELL, J. D. C. (1967) Electron microscopy and electron diffraction. In J. Zussman (ed.), *Physical Methods in Determinative Mineralogy*. Academic Press, N. Y., 514 p.
- ROGERS, A. F., AND P. F. KERR (1942) *Optical Mineralogy*. McGraw-Hill Book Co., N. Y., 390 p.

Manuscript received, December 10, 1969; accepted for publication, January 7, 1972.